Available online at www.sciencedirect.com

ScienceDirect

Advances in Space Research 65 (2020) 763–771

ADVANCES IN SPACE RESEARCH (a COSPAR publication)

www.elsevier.com/locate/asr

RadioAstron reveals super-compact structures in the bursting H_2O maser source G25.65+1.05

O.S. Bayandina [a,*], N.N. Shakhvorostova [a,b], A.V. Alakoz [a], R.A. Burns [c], S.E. Kurtz [d], I.E. Val'tts [a]

[a] Astro Space Center, Lebedev Physical Institute, Russian Academy of Sciences, 84/32 Profsoyuznaya st., Moscow, GSP-7, 117997, Russia
[b] Astronomical Observatory, Institute for Natural Sciences and Mathematics, Ural Federal University, 19 Mira Street, Ekaterinburg 620002, Russia
[c] Mizusawa VLBI Observatory, National Astronomical Observatory of Japan, 2-21-1 Osawa, Mitaka, Tokyo 181-8588, Japan
[d] Instituto de Radioastronomía y Astrofísica, Universidad Nacional Autónoma de México, Morelia 58090, Mexico

Received 14 December 2018; received in revised form 26 February 2019; accepted 10 March 2019
Available online 20 March 2019

Abstract

Water masers are well-known to be variable on a variety of time scales, but only three Galactic H_2O masers are known to flare to the level of 10^5–10^6 Jy ($T_B \sim 10^{17}$ K): Orion KL, W49N, and the recently discovered G25.65+1.05. Recently detected flaring activity of H_2O maser in the massive star-forming region G25.65+1.05 gave us a unique opportunity to study the fine structure of H_2O maser emission in the bursting state with extremely high space VLBI angular resolution. Observation of the source was carried out with ~9 Earth diameter space-ground baseline within the framework of the RadioAstron project. H_2O maser emission from two spectral features, including the bursting one, was detected in the experiment. Only ~1% of the bursting H_2O maser emission was detected on the space-ground baselines: it indicates the presence of a very compact spatial structure with a size of ~25 μas, which corresponds to 0.05 AU or ~5 solar diameters at the distance to the source of 2.08 kpc, and the brightness temperature of $\sim 3 \times 10^{16}$ K. Analysis of the flux density as a function of the baseline length for the bursting H_2O maser feature in the source shows that most of the emission comes from an extended "halo" structure, while the core of emission is very compact and has an extreme brightness temperature. These results are in agreement with the model of interacting maser clouds considered as the likely explanation of the nature of the burst in the source. Under the assumption of such a model, the beam size of maser emission is reduced while the brightness temperatures similar to the highest observed values are produced.

Keywords: Stars: formation; Masers; Instrumentation: high angular resolution

1. Introduction

Cosmic water masers were discovered nearly 50 years ago (Knowles et al., 1969), and in that time they have become a powerful, multi-purpose tool: an astrometric tracer of galactic structure, a mass-detector for black holes, and a probe of star formation regions, locating deeply embedded massive young stellar objects, and pinpointing accretion disks and molecular outflows associated with star formation.

These masers are not only a powerful diagnostic tool, they are also intriguing objects for study in their own right. One phenomenon, as yet unexplained, is "super-bursts" of water maser emission observed in Orion KL (e.g. Omodaka et al., 1999; Matveyenko et al., 1998) and in W49N (e.g. Abramian et al., 1983; Tolmachev, 2014). In recent years the H_2O maser source in the massive star-

* Corresponding author.
E-mail address: bayandina@asc.rssi.ru (O.S. Bayandina).

https://doi.org/10.1016/j.asr.2019.03.011
0273-1177/

forming region G25.65+1.05 (IRAS 18316-0602, Mol 62, RAFGL 7009S) has undergone several powerful flares (Lekht et al., 2018; Volvach et al., 2019). The source was included in the single-dish telescope monitoring programs, using Pushchino RT-22 m and Simeiz RT-22 m, and showed five strong H_2O maser flares with increasing flaring flux density and decreasing period between events – see Table 1.

The huge flux densities of the recent bursts placed G25.65+1.05 on a par with such outstanding "superburst" sources as Orion KL and W49N. But in contrast to them, the source is much less known and did not attract much attention before.

The distance to the source is an open question, which complicates the comparison of the absolute flux densities of the burst in G25.65+1.05 and other sources. In our study we accept the distance to the source of 2.08±0.37 kpc calculated on the basis of The Bar and Spiral Structure Legacy (BeSSeL) Survey data (Reid et al., 2016; BeSSeL Survey web-page, 2019).

There are no VLBI images of H_2O maser emission in the field from a pre-burst epoch. Shortly after the burst of December 2016 two related proposals were submitted to space VLBI project RadioAstron and to the Very Long Baseline Array (VLBA) for simultaneous observations of G25.65+1.05. The simultaneous RadioAstron and VLBA observation of G25.65+1.05 was carried out in August 2017 with a space-ground baseline length of ~3 Earth diameters (ED); this was the very first VLBI study of 22 GHz H_2O maser in the source (Bayandina et al. 2019, in preparation). Good coverage achieved in the session allowed us to obtain a detailed high-resolution map of the H_2O maser emission in the field. However, the observation occurred at a non-bursting epoch (between bursts of December 2016 and September 2017) when H_2O maser showed a stable state flux density of ~500 Jy (see single-dish monitoring on this epoch in Shakhvorostova et al., 2018).

In contrast, the second RadioAstron session was conducted shortly after the burst of September 2017 when the source was still flaring with flux density of ~13,000 Jy. In this observation the significantly longer projected space-ground baseline length of ~9 ED was achieved. In this paper we describe the first and quite possibly the only study of H_2O maser source in the bursting state with the ultra-high angular resolution of the space VLBI.

The detection of G25.65+1.05 with ~9 ED baseline is very close to the RadioAstron record in angular resolution for galactic H_2O masers. The current record is the detection of W49N with projected space-ground baselines of about 9.6 ED and angular resolution of ~23 μas (~30 solar diameters considering a distance to the source of about 11 kpc) (Kardashev and Kovalev, 2015; Shakhvorostova et al., 2018). The record in linear resolution belongs to Cepheus A and it is about 1 solar diameter (two unresolved components smaller than 15 μas were detected with the projected space-ground baseline of 3.3 ED and resolution of ~66 μas) (Sobolev et al., 2018).

2. Observations

The observation of massive star-forming region G25.65+1.05 was carried out on September 29, 2017 in the framework of space VLBI project RadioAstron (Kardashev et al., 2017) with the 10-m Space Radio Telescope (SRT) and two ground-based telescopes: 32-m radio telescope of the Toruń Centre for Astronomy of Nicolaus Copernicus University (Tr, Toruń, Poland) and 26-m radio telescope of the Hartebeesthoek Radio Astronomy Observatory (Hh, Johannesburg, Republic of South Africa).

The session was held in a period from 12:00 UT to 16:00 UT – the SRT participated in the 50 min segment from 13:10 UT to 14:00 UT with 570 s scans; in the remaining time the ground-based telescopes observed in phase-referencing mode with ~1 min scans. Observation in phase-referencing mode was planned with the expectation of broader ground-based telescope support; due to last minute scheduling conflicts, only two ground telescopes observed.

Position of H_2O maser emission peak detected in G25.65+1.05 on pre-burst epoch with VLA A-configuration (NRAO archive data of the project AS815 22-Sept-2004, unpublished) was used as the pointing coordinates: RA (J2000) = $18^h34^m20.90^s$, DEC(J2000) = $-05°59'41.46''$. Only the target source was observed on the space-ground baselines – no calibrators were observed with SRT, because of technical restrictions on the duration of this observing session and slow slewing between the target and possible

Table 1
Summary of the detected H_2O maser flares in G25.65+1.05.

#	Date	Flux density (Jy)	Telescope	Reference
1	13 Jun 2002	~3400	RT-22 of the Pushchino Radio Astronomy Observatory	[1]
2	26 Aug 2010	~19,000	RT-22 of the Pushchino Radio Astronomy Observatory	[1]
3	12 Dec 2016	~46,000	RT-22 of the Pushchino Radio Astronomy Observatory	[1]
4	16 Sep 2017	~65,000	RT-22 of the Crimean Astrophysical Observatory	[2]
5	20 Nov 2017	~76,000	RT-22 of the Pushchino Radio Astronomy Observatory	[3]

Note: [1] (Lekht et al., 2018), [2] (Volvach et al., 2019), [3] (Ashimbaeva et al., 2017).

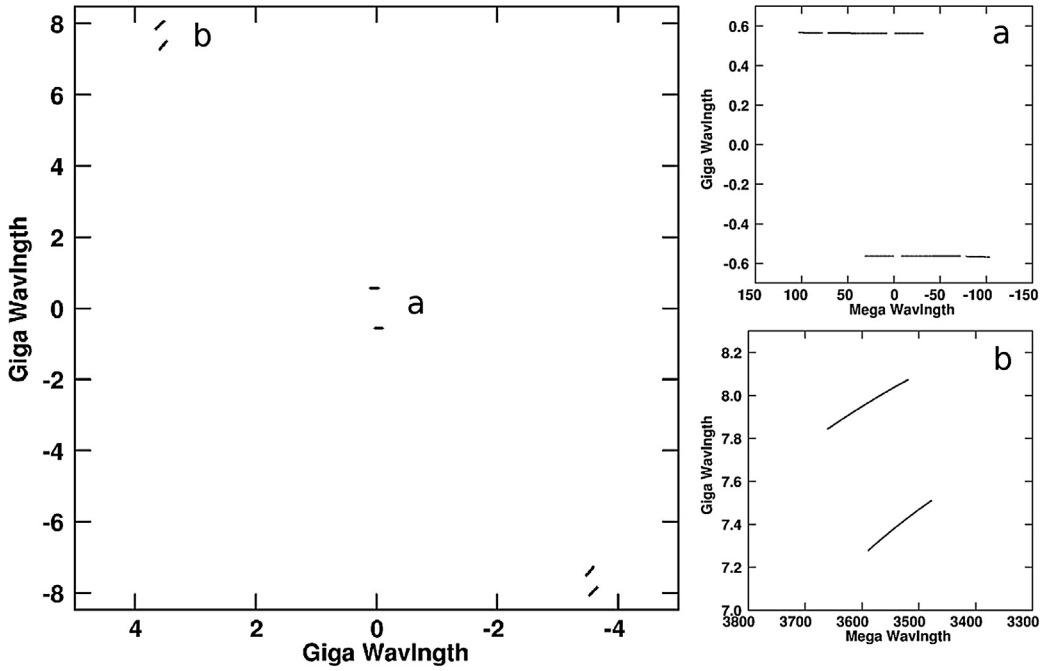

Fig. 1. Left panel: The uv-plane coverage plotted for the whole observing period from 12:00 to 16:00 UT. Right panel: Zoom into the uv-plane coverage for (a) the Tr-Hh ground baselines and (b) the SRT-Tr and SRT-Hh space-ground baselines. The uv-plane coverage for space-ground baselines corresponds to the SRT observing time 13:10–14:00 UT.

Table 2
Observation parameters summary.

Baseline	Baseline length (km)	Baseline length (ED)	Angular res. (μas)	Pos. angle (°)
Hh-Tr	8108	0.64	340	4.7–7.2
SRT-Tr	~109,500	8.51–8.67	~25.5	25.0–26.1
SRT-Hh	~116,500	9.07–9.22	~23.9	23.7–24.9

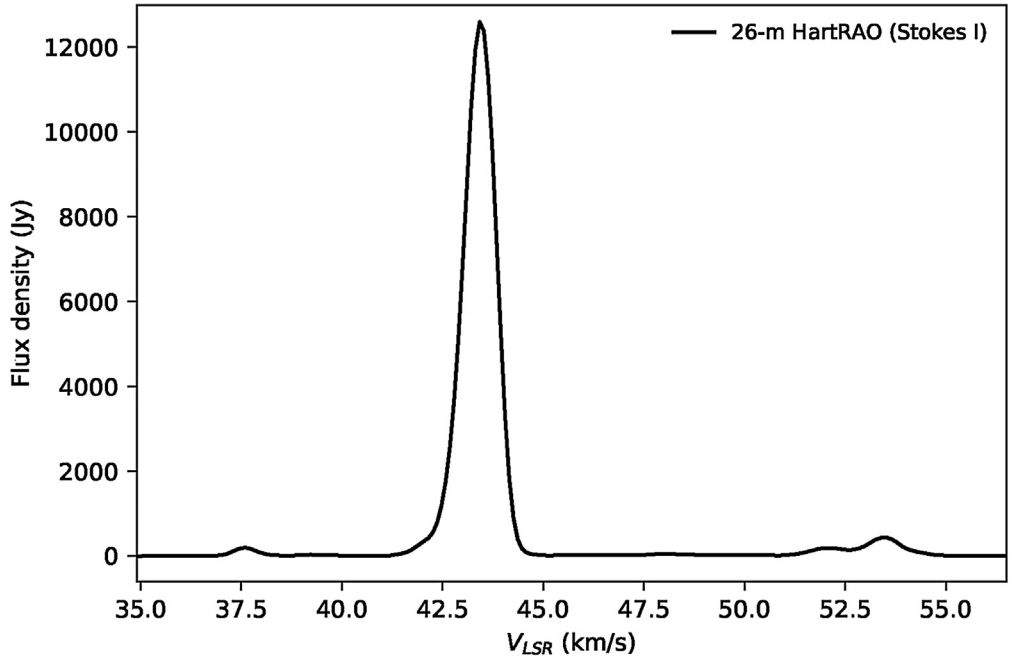

Fig. 2. The single-dish spectrum of 22 GHz maser emission in G25.65+1.05 obtained on the date of RadioAstron observations (2017 Sep 29) with 26-m radio telescope of the Hartebeesthoek Radio Astronomy Observatory. Spectrum of the source contains three groups of spectral features, hereinafter referred to as: blue spectral feature – V_{LSR} ~37 km/s, bursting spectral feature – V_{LSR} ~42 km/s, and red spectral feature – V_{LSR} ~51–55 km/s.

calibrator source. In the ground array segment of the session, two calibrator sources were included: fringe finder B1730-130 was observed every 1 h and the phase reference source J1818-050 (RA(J2000) = $18^h21^m11.8095^s$, DEC (J2000) = $-05°02'20.086''$) was observed for 27 s between of ~1 min target source scans.

The uv-coverage plot for the session is shown in Fig. 1. During the space VLBI segment the uv-coordinates of the SRT-Hh baseline changed from (3.62, 7.76) to (3.47, 7.98) and of the SRT-Tr baseline – from (3.55, 7.20) to (3.43, 7.43) in units of Giga-wavelengths. An observation parameters summary is presented in Table 2.

The observations were performed in K-band (with the central frequency of 22.228 GHz) in two polarizations (LCP and RCP) with a total bandwidth of 32 MHz per polarization (two sub-bands of 16 MHz each) with frequency resolution of 7.81 kHz, corresponding to spectral resolution of 0.11 km/s. But only the right-hand circular polarization data is presented since observation at 32-m Toruń radio telescope was performed in single polarization mode.

3. Data reduction & results

Correlation of the data was made using the software correlator of the Astro Space Center (ASC) of the Lebedev Physical Institute (Likhachev et al., 2017). The orbital parameters of SRT were provided with the accuracy of 500 m in position and 0.02 m/s in velocity (Kardashev et al., 2013).

The very limited number of telescopes participating in the observation (the space VLBI segment of our observation consists of three telescopes) and poor uv-plane coverage limits us in the use of standard calibration techniques and does not allow us to perform imaging.

In order to get maximum results from our limited data set, we performed the post-correlation data reduction using two software packages: AIPS (Astronomical Image Processing System, AIPS web-page, 2019) and PIMA (PIMA web-page, 2019). The main data reduction steps were performed with the Astronomical Image Processing System (AIPS) software package. An additional fringe search was done using the software package PIMA (Petrov et al., 2011). This package provides crucial for Space VLBI data processing capabilities: its fringe-fitting procedure searches not only over the residual delay and fringe rate, but also over an acceleration term – which is important since there is some inaccuracy of measurements of the SRT's orbit. But the package, originally designed for astrometric and geodetic applications, lacks spectral data processing capabilities.

The fringe finder B1730-130 wasn't observed with SRT, so it was not possible to calibrate the residual delays. The residual rates were calculated using the target source data with solution intervals of ~1 min.

A priori amplitude calibration was made using the "template spectrum" method with AIPS task ACFIT. The method is useful for high frequency VLBI observations when instrumental effects are relatively unstable or not well known (see, for example, Doeleman et al., 2001). The template total power spectrum of Hh was fitted to the total power spectra of two other antennas to determine their SEFD as a function of time. The single-dish data obtained with the Hh telescope on the date of RadioAstron session (see Fig. 2) was used to scale the template spectrum. Note that according single-dish monitoring detected flux densities of maser emission differs in the right and left polarizations by less than 2%.

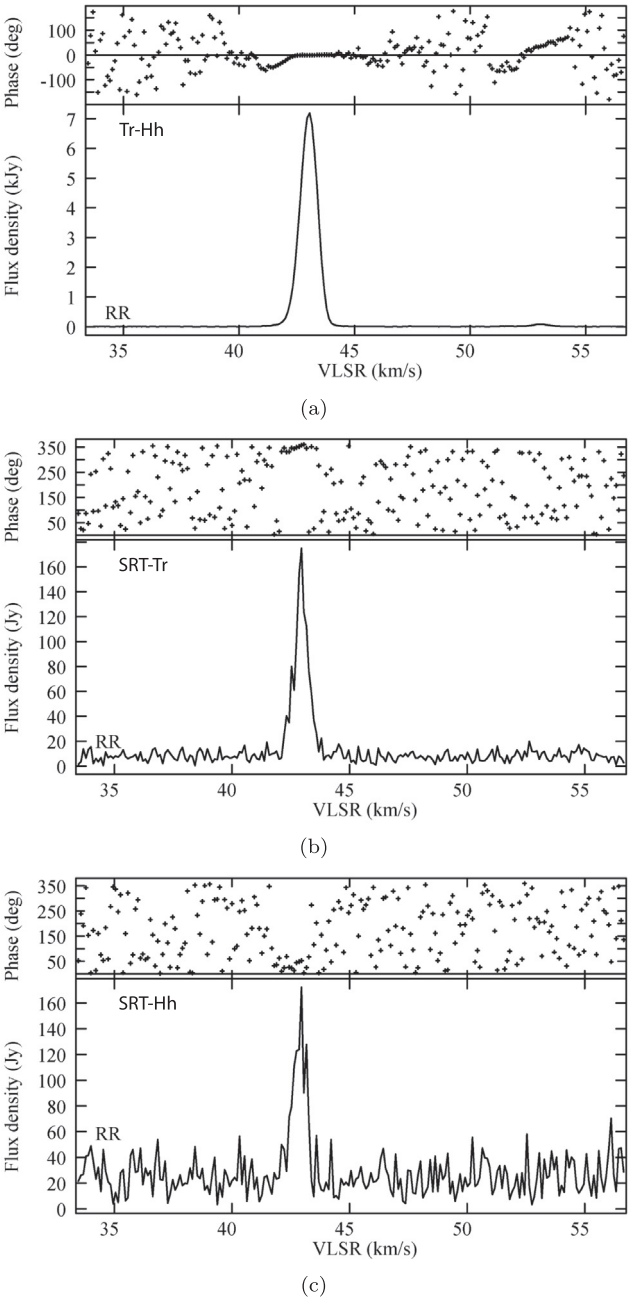

Fig. 3. Cross-correlation vector averaged spectra of 22 GHz maser emission detected on (a) ground-ground baseline Tr-Hh, and space-ground baselines (b) SRT-Tr & (c) SRT-Hh.

Fig. 3 shows the calibrated with AIPS (no residual delay correction) cross-correlation vector averaged spectra detected with ground-ground (Tr-Hh) and space-ground (SRT-Tr, SRT-Hh) baselines. On the space-ground baselines of ~9 ED the signal is detected from two spectral features: the bursting spectral line at the velocity of ~43 km/s and the redshifted feature at the velocity of ~53 km/s. Close-up on cross-correlation spectra for the redshifted feature is presented on Fig. 4.

On the ground-ground baseline of ~1 ED the correlated flux density of the bursting spectral feature is ~7000 Jy, which is approximately 60% of the single-dish flux detected on the same day with 26-m HartRAO radio telescope. In contrast, on the space-ground baselines of ~9 ED the flux density is ~160 Jy, i.e. only ~1% of the source flux density is recovered (see Table 3).

The redshifted feature at the velocity of ~53 km/s shows a lower flux density loss on the ground-ground baseline – 70% of the single-dish flux density is recovered. The detection on the space-ground baselines is marginal for this feature, but there is still ~7% of the single-dish flux density (see Table 3).

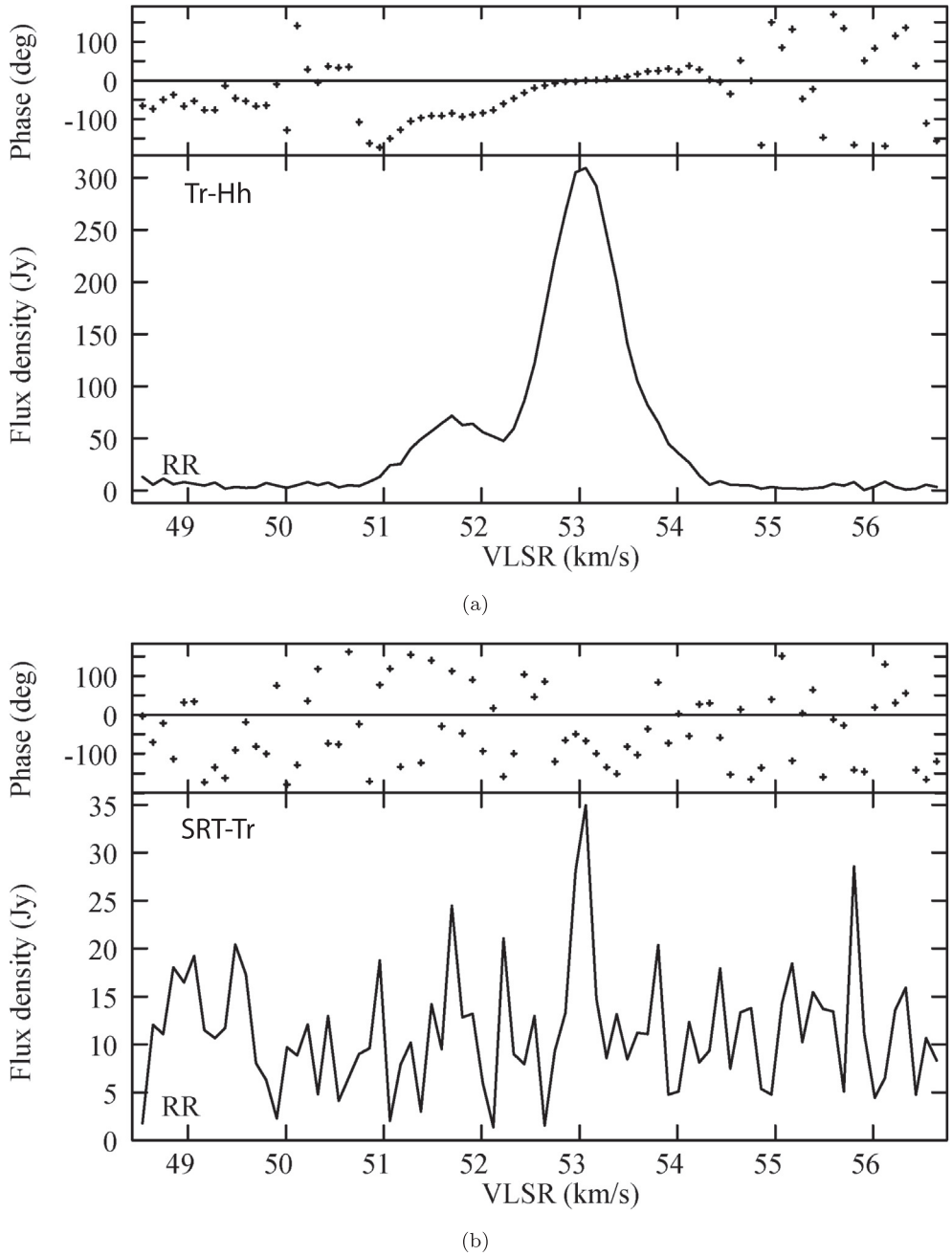

Fig. 4. Cross-correlation vector averaged spectra of 22 GHz maser emission from redshifted spectral feature at ~53 km/s detected on (a) ground-ground baseline Tr-Hh and (b) space-ground baselines SRT-Tr.

Table 3
Correlated flux densities of the detected spectral features at different baselines.

V_{peak} (km/s)	ΔV (km/s)	Baseline	Correlated flux density (Jy)	Recovered flux density (%)
The bursting maser feature				
43.42	0.79	Hh	12,315 ± 31	100
43.02	0.74	Hh-Tr	7220 ± 18	59
42.94	0.65	SRT-Tr	165 ± 4	1.3
42.89	0.68	SRT-Hh	159 ± 13	1.3
The redshifted maser feature				
53.47	0.87	Hh	420 ± 9	100
53.05	0.77	Hh-Tr	302 ± 5	72
53.04	0.23	SRT-Tr	∼30	∼7
–	–	SRT-Hh	–	–

Plots of the visibility amplitude against projected baseline length for the two detected spectral features at ∼43 km/s and ∼53 km/s are shown on Fig. 5. On the plots, gray points represent the corresponding single-dish flux density, black points – the correlated flux densities at the ground-ground and space-ground baselines from Table 4. With a few visibility measurements, we can only say that the features probably have a structure of two or more components, the most compact of which is unresolved at the fringe spacing of ∼25 μas.

Assuming a two-component structure of the emitting area, i.e. extended halo and compact core, we can estimate angular sizes and averaged brightness temperatures of these two components from their visibilities (see, for example, (Lobanov, 2015) for details). We used a Gaussian function to fit the visibility measurements obtained in our observations. Gray and black curves on Fig. 5 represent Gaussian fits for extended (halo) and compact (core) components respectively. We also perform the fitting with ground VLBI and space VLBI visibilities (black dashed line) in order to get estimates for the most compact "core" of emission. Results of these simple approximations are given in Table 4.

4. Discussion

Despite the active study of maser sources, the nature of maser "bursts" still remains an enigma. This is largely due to the rarity and transience of such phenomena, as well as the very limited sample of flaring sources.

Various mechanisms have been proposed to explain the nature of maser bursts: proto-planetary rings seen edge-on (Matveenko et al., 1988), shock waves induced by an outflow (Garay et al., 1989), interacting maser clouds (Deguchi and Watson, 1989; Boboltz et al., 1998), accretion bursts (Moscadelli et al., 2017), and most recently, superradiance and entangled quantum states (Rajabi and Houde, 2017). There seems to be no universal answer – it is quite possible that different mechanisms are at work in different sources.

In the case of G25.65+1.05, single-dish (Lekht et al., 2018; Volvach et al., 2019), VLA (Bayandina et al., 2019) and ground VLBI (Bayandina et al. 2019, in preparation; Burns et al. 2019, in preparation) observations of the source made it possible to reduce the list of putative H_2O maser burst models. Non-detection of significant flares or spatial structure changes in other maser species in the region (Bayandina et al., 2019) indicates that the bursts had a local character and were not related to a rise of activity of the entire source. The maser flares in the source are short-lived and the flaring maser feature remains unsaturated (Lekht et al., 2018; Volvach et al., 2019) which suggests that the bursts are related to the internal structure of the H_2O maser, and not to changes in the maser environment or pumping.

Hence, an investigation of the spatial structure of the H_2O maser in G25.65+1.05 may be the key. High-resolution VLBI observations can reveal the complex fine structure of H_2O masers, which agrees well with the idea that there are fine masing spots overlapping occasionally within a maser cloud (Deguchi and Watson, 1989). Detection of fine (double) structure in the flaring sources Orion KL and W49N are described, for example, in Boboltz et al. (1998) and Shimoikura et al. (2005). But recent space VLBI RadioAstron detection of double structure of a single (according to ground baseline observations) maser spot in Cepheus A seems to be well-explained as "vortices caused by flow around an obstacle", rather than two chance overlapping clouds (Sobolev et al., 2018).

The inclusion of the Space Radio Telescope allows us to go further and get a unique estimate of the size of the emitting region. The detection of the emission from the bursting feature in G25.65+1.05 on space-ground baselines of 9 ED indicates that there are super-compact H_2O maser features with a size of ∼25 μas, which corresponds to 0.05 AU or ∼5 solar diameters at the distance of 2.08±0.37 kpc. Analysis of the flux density as a function of the baseline length for the bursting H_2O maser feature in the source shows that the most of the emission comes from an extended "halo" structure, while the core of emission is very compact and has an extreme brightness temperature of $\sim 10^{16}$ K.

These results are in general agreement with the model of interacting maser clouds (Deguchi and Watson, 1989; Boboltz et al., 1998), which we consider as a likely explanation of the nature of the burst in the source. Under the assumption of such a model the beam size of maser emission is reduced while extreme brightness temperatures are produced (Deguchi and Watson, 1989) – the overlap region is quite small (smaller than size of individual maser spots) while the brightness temperature is higher for observers within the beam.

Ground VLBI observations of G25.65+1.05 (Bayandina et al. 2019, in preparation; Burns et al. 2019, in preparation) revealed a double structure of the bursting feature with two milliarcsecond-scale components interacting at a NW-SE orientation. Unfortunately, our RadioAstron observation has very limited resolution in NW-SE direction

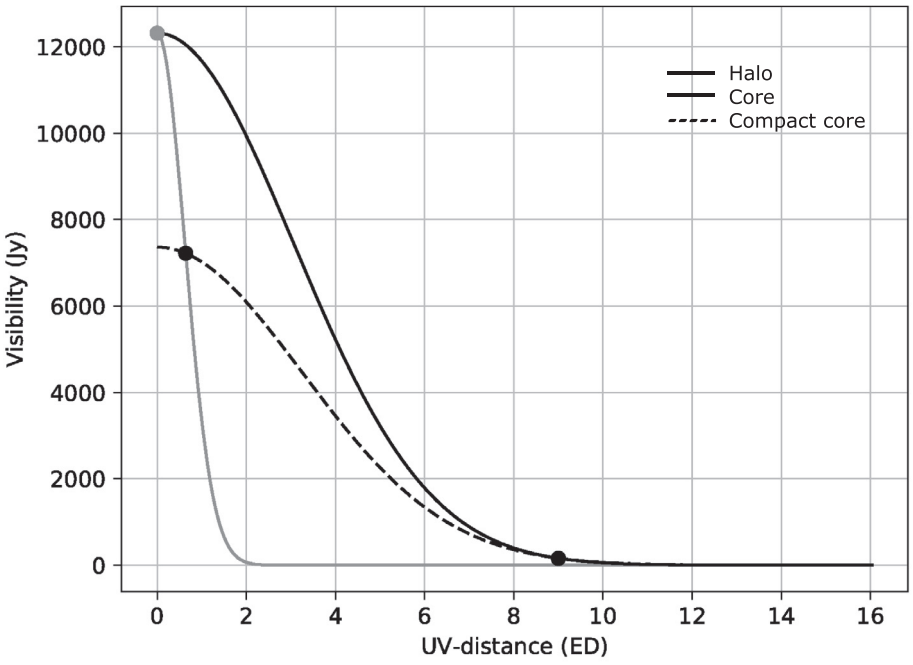

(a)

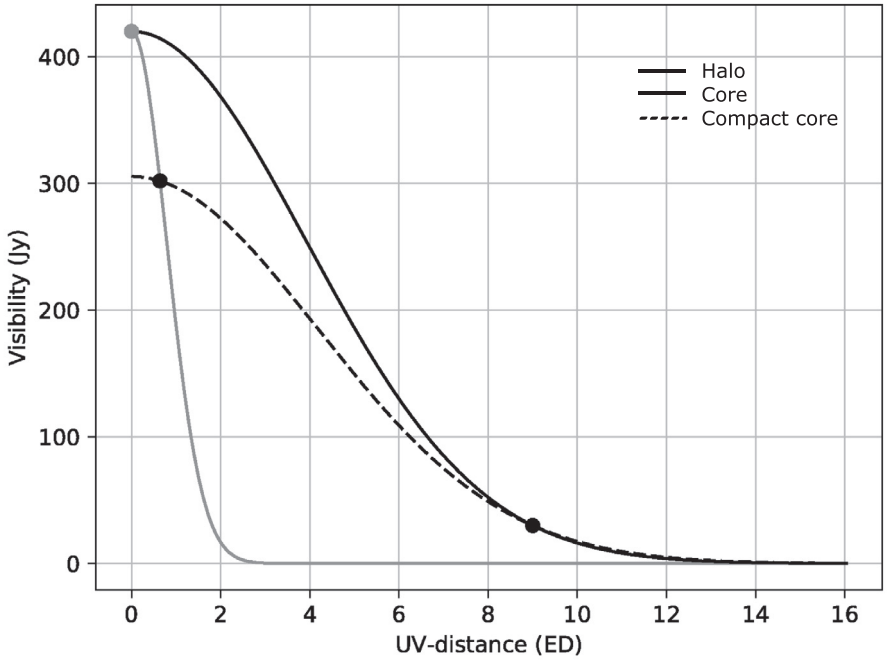

(b)

Fig. 5. Visibility amplitude vs. baseline length for (a) the bursting maser line at the velocity of ~43 km/s and (b) the redshifted feature at the velocity of ~53 km/s.

(see Fig. 1), what does not allow us to study the structure of the bursting feature in this slice. Note that the presented estimates of the sizes of detected with RadioAstron maser features are convenient only for NE-SW direction.

The detection of the non-bursting redshifted spectral feature with the space-ground baseline enables additional analysis – we can not only estimate the bursting feature parameters, but also compare them with those obtained for a "stable" feature. The redshifted feature at ~53 km/s is known to be variable, but not flaring (Lekht et al., 2018) and the total flux density detected in RadioAstron session is considered to be a typical value for it.

Imaging of the source with ground interferometric arrays (Bayandina et al., 2019) with mas-resolution shows

Table 4
Estimates of the angular size and average brightness temperature of structural components of two detected features.

V_{LSR} (km/s)	Component	Angular size (μas)	Brightness temperature (K)
43	Halo	133	1.7×10^{15}
	Core	27	4.2×10^{16}
	Compact core	25	2.9×10^{16}
53	Halo	105	9.6×10^{13}
	Core	21	2.4×10^{15}
	Compact core	20	2.0×10^{15}

that both features, detected in our RadioAstron observations, are associated with the same objects – they are parts of an arc-shaped H_2O maser clusters possibly tracing a young shock driven from one of the continuum sources detected in the region.

Despite significant differences in the behavior of two detected maser features – bursting and non-bursting – the results obtained for them in this experiment are seems to be quite similar (see Table 4 and Fig. 5). Both features show the presence of an extended halo emission (detectable in single-dish observations, but resolved with ground VLBI resolution) coming from a region of the size ~100 μas. But in the case of the bursting feature the size of a halo is ~20% larger and the brightness temperature of an emitting region is about two orders of magnitude higher.

Moving from extended to compact emission ("Core" estimates in Table 4), both features reveal an identical 5× drop in the size of the emitting area and 25× increase of brightness temperature. The estimates for the bursting feature remain higher than for the non-bursting one: the size of the "core" of the bursting emission is ~20% larger with about an order of magnitude higher brightness temperature. Since in this "Core" approximation we do not use ground VLBI visibilities, we accept it as a reference model estimate.

A more accurate calculation of the most compact "core" emission parameters ("Compact core" estimates in Table 4), based on the ground and space VLBI visibilities, shows a slightly greater difference between "core" and "compact core" values for the bursting feature, the values for the red feature stay almost constant. This may indicate that the redshifted spectral feature is almost resolved with space VLBI baseline, while the bursting feature could have a more complex structure. In summary, both detected on the space-ground baselines features appears to be almost equally compact in NE-SW direction, but the bursting feature shows 10 times higher brightness temperature and more extended "halo" emission.

RadioAstron observations of Cepheus A revealed that H_2O maser emission originates from spatial regions with as fine size as 1 solar diameter (Sobolev et al., 2018). Note that Cepheus A spectral feature studied in (Sobolev et al., 2018) showed a rise of flux density at the time of RadioAstron session and the authors pointed out that the epoch of observation could be pre- or post-burst. Considering the (Sobolev et al., 2018) study, we can assume that the H_2O maser features detected on space-ground baselines in G25.65+1.05 could still be unresolved even with the baseline of 9 ED, since the achieved resolution probes a region of the size of ~5 solar diameters.

Further analysis of VLBI and single-dish monitoring data on the flaring epoch for G25.65+1.05 will provide new clues on the nature of the H_2O maser bursts in the source and help us to interpret the unique RadioAstron detection described in this paper.

5. Conclusions

Space VLBI observations of the bursting H_2O maser G25.65+1.05 were carried out during the active state epoch. During observations of H_2O masers in the G25.65 +1.05 using the ground-space interferometer with the 10-m space radio telescope RadioAstron and relatively small ground antennas, signal from the source was detected on projected baselines ~9 ED.

1. On the space-ground baselines the signal was detected from two spectral features: the bursting spectral feature at the velocity of ~43 km/s and the non-bursting feature with velocity of ~53 km/s.
2. Estimated size of the bursting maser feature at the velocity ~43 km/s detected at space-ground baselines is ~25 μas with a brightness temperature T_B ~2.9×10^{16} K.
3. Obtained results are in agreement with an overlapping clouds model of the burst.

Acknowledgments

The RadioAstron project is led by the Astro Space Center of the Lebedev Physical Institute of the Russian Academy of Sciences and the Lavochkin Scientific and Production Association under a contract with the Russian Federal Space Agency, in collaboration with partner organizations in Russia and other countries.

This work is based in part on observations carried out using the 32-meter radio telescope operated by Toruń Centre for Astronomy of Nicolaus Copernicus University in Toruń, Poland (supported by the Polish Ministry of Science and Higher Education SpUB grant) and 26-meter radio telescope operated by Hartebeesthoek Radio Astronomy Observatory in Johannesburg, Republic of South Africa. We are grateful to the astronomy observatories for the opportunity to observe with the radio telescopes and to the staff of the observatories for their assistance in carrying out the observations.

Special thanks to RT-26 HartRAO and personally to G. C. MacLeod for providing single-dish data on the date of RadioAstron observations.

References

Abramian, L.E., Venger, A.P., Gosachinskij, I.V., bvKandalian, R.A., Martirosian, R.M., Sanamian, V.A., Yudaeva, N.A., 1983. A flare of the H_2O radio line emission in W49. Astrofyzika 19, 830–834.

AIPS web-page, 2019. Available at: <http://www.aips.nrao.edu> (accessed 13 February 2019).

Ashimbaeva, N.T., Platonov, M.A., Rudnitskij, G.M., Tolmachev, A.M., 2017. The H_2O Maser G25.65+1.05 Flared Again, ATel #11042. <http://www.astronomerstelegram.org/?read=11042>.

Boboltz, D.A., Simonetti, J.H., Dennison, B., Diamond, P.J., Uphoff, J. A., 1998. A water maser flare in W49N: amplification by a rotating foreground cloud. ApJ 509, 256–261. https://doi.org/10.1086/306482.

Bayandina, O.S., Burns, R.A., Kurtz, S.E., Shakhvorostova, N.N., Val'tts, I.E. 2019, JVLA overview of the bursting H_2O maser source G25.65+1.05, arXiv:<1812.11353>. 2018arXiv181211353B.

BeSSeL Survey web-page, 2019. Available at: <http://bessel.vlbi-astrometry.org> (accessed 25 February 2019).

Deguchi, S., Watson, W.D., 1989. Interacting masers and the extreme brightness of astrophysical water masers. ApJ Lett. 340, L17–L20. https://doi.org/10.1086/185428.

Doeleman, S.S., Shen, Z.-Q., Rogers, A.E.E., Bower, G.C., Wright, M.C. H., Zhao, J.H., et al., 2001. Structure of Sagittarius A^* at 86 GHZ using VLBI closure quantities. AJ 121, 2610–2617. https://doi.org/10.1086/320376.

Garay, G., Moran, J.M., Haschick, A.D., 1989. The Orion-KL super water maser. ApJ 338, 244–261. https://doi.org/10.1086/167195.

Kardashev, N.S., Khartov, V.V., Abramov, V.V., Avdeev, V.Yu., Alakoz, A.V., Aleksandrov, Yu.A., Ananthakrishnan, S., Andreyanov, V.V., Andrianov, A.S., et al., 2013. "RadioAstron" – A telescope with a size of 300 000 km: main parameters and first observational results. Astron. Rep. 57, 153–194. https://doi.org/10.1134/S1063772913030025.

Kardashev, N.S., Kovalev, Y.Y., 2015. Ultra-high spatial resolution image of nearby radio galaxy 3C 84 at 22GHz, RadioAstron Newsletter Number 29, <http://www.asc.rssi.ru/radioastron/news/newsl/en/newsl_29_en.pdf>.

Kardashev, N.S., Alakoz, A.V., Andrianov, A.S., Artyukhov, M.I., Baa, W., Babyshkin, V.E., Bartel, N., Bayandina, O.S., Val'tts, I.E., Voitsik, P.A., et al., 2017. RadioAstron science program five years after launch: main science results. Sol. Syst. Res. 51, 535–554. https://doi.org/10.1134/S0038094617070085.

Knowles, S.H., Mayer, C.H., Cheung, A.C., Rank, D.M., Townes, C.H., 1969. Spectra, variability, size, and polarization of H_2O microwave emission sources in the galaxy. Science 163, 1055–1057. https://doi.org/10.1126/science.163.3871.1055.

Lekht, E.E., Pashchenko, M.I., Rudnitskij, G.M., Tolmachev, A.M., 2018. Superflares of H_2O maser emission toward the protostellar object G25.65+1.05 (IRAS 18316-0602). Astron. Rep. 62, 213–224. https://doi.org/10.1134/S1063772918030071.

Likhachev, S.F., Kostenko, V.I., Girin, I.A., Andrianov, A.S., Rudnitskiy, A.G., Zharov, V.E., 2017. Software correlator for radioastron mission. J. Astr. Inst. 6, 1750004. https://doi.org/10.1142/S2251171717500040.

Lobanov, A.P., 2015. Brightness temperature constraints from interferometric visibilities. A&A 574. https://doi.org/10.1051/0004-6361/201425084, id A84 9 pp.

Matveenko, L.I., Graham, D.A., Diamond, P.J., 1988. The H_2O maser flare region in the Orion-Kl nebula. Sov. Astron. Lett. 14, 468–476.

Matveyenko, L.I., Diamond, P.J., Graham, D.A., 1998. Discovery of a jet in the region of H_2O supermaser emission in Orion KL. Astron. Lett. 24, 623–631.

Moscadelli, L., Sanna, A., Goddi, C., Walmsley, M.C., Cesaroni, R., Caratti o Garatti, A., Stecklum, B., Menten, K.M., Kraus, A., 2017. Extended CH_3OH maser flare excited by a bursting massive YSO. A&A 600 (id L8), 5. https://doi.org/10.1051/0004-6361/201730659.

Omodaka, Toshihiro, Maeda, Toshihisa, Miyoshi, Makoto, et al., 1999. The enormous outburst of the 7.9 km/s water-maser feature in Orion KL. PASJ 51, 333–336. https://doi.org/10.1093/pasj/51.3.333.

Petrov, L., Kovalev, Y.Y., Fomalont, E.B., Gordon, D., 2011. The very long baseline array galactic plane survey – VGaPS. AJ 142 (2), 23. https://doi.org/10.1088/0004-6256/142/2/35, article id 35.

PIMA web-page, 2019. Available at: <http://astrogeo.org/pima/> (accessed 25 February 2019).

Rajabi, F., Houde, M., 2017. Explaining recurring maser flares in the ISM through large-scale entangled quantum mechanical states. Sci. Adv. 3 (3), e1601858. https://doi.org/10.1126/sciadv.1601858.

Reid, M.J., Dame, T.M., Menten, K.M., Brunthaler, A., 2016. A parallax-based distance estimator for spiral arm sources. ApJ 823, 77. https://doi.org/10.3847/0004-637X/823/2/77.

Shakhvorostova, N.N., Alakoz, A.V., Sobolev, A.M., 2018. Brightness temperatures of galactic masers observed in the RadioAstron project. In: Tarchi, A., Reid, M.J., Castangia, P. (Eds.), Proceedings of the International Astronomical Union S336 "Astrophysical Masers: Unlocking the Mysteries of the Universe, vol. 13. Cambridge University Press, (United Kingdom), pp. 447–448. https://doi.org/10.1017/S174392131701047X, arXiv:<1802.05120>.

Shakhvorostova, N.N., Vol'vach, L.N., Vol'vach, A.E., Dmitrotsa, A.I., Bayandina, O.S., Val'tts, I.E., Alakoz, A.V., Ashimbaeva, N.T., Rudnitskii, G.M., 2018. Search for H_2O maser flares in regions of formation of massive stars. Astron. Rep. 62, 584–608. https://doi.org/10.1134/S1063772918090081.

Shimoikura, T., Kobayashi, H., Omodaka, T., Diamond, P.J., Matveyenko, L.I., Fujisawa, K., 2005. VLBA observations of a bursting water maser in Orion KL. ApJ 634, 459–467. https://doi.org/10.1086/432865.

Sobolev, A.M., Moran, J.M., Gray, M.D., Alakoz, A., Imai, H., Baan, W. A., Tolmachev, A.M., Samodurov, V.A., Ladeyshchikov, D.A., 2018. Sun-sized water vapor masers in Cepheus A. ApJ 856 (1), 9. https://doi.org/10.3847/1538-4357/aab096, article id 60.

Tolmachev, A. 2014. A Flare of the Violet Component of H_2O Maser in W49N, ATel #5826. <http://www.astronomerstelegram.org/?findmsg>.

Volvach, L.N., Volvach, A.E., Larionov, M.G., MacLeod, G.C., van den Heever, S.P., Wolak, P., Olech, M., 2019. Powerful bursts of water masers towards G25.65+1.05. MNRAS 482, L90–L92. https://doi.org/10.1093/mnrasl/sly193.